PUNCHING SHEAR STRENGTH OF FLAT SLAB EDGE COLUMN CONNECTIONS WITH OUTWARD ECCENTRICITY OF LOADING

Nivea G. B. Albuquerque, Guilherme S. Melo and Robert L. Vollum

Biography: Nivea G. B. Albuquerque is a Civil Engineer who received her PhD from the University of Brasilia, Brazil, and was awarded in Brazil for the best PhD Thesis in the field of Civil Engineering in 2014. She is a Postdoctoral Research Fellow at the University of Brasilia.

ACI Member **Guilherme S. Melo** is Professor at the University of Brasilia, Brazil. He is a member of ACI Committees 440, Fiber-Reinforced Polymer Reinforcement; and Joint ACI-ASCE Committee 445, Shear and Torsion. His research interests include punching and post-punching of flat plates and the strengthening and rehabilitation of structures.

ACI Member **Robert L. Vollum** is a Reader at Imperial College London, UK. He is a member of British Standards Committee 525/2 for Structural Concrete, Task Group 4 of Working Group 1 of CEN/TC 250/SC 2 Shear, Punching and Torsion, fib WP 2.2 Ultimate Limit State Design and fib WP 2.2.3 Punching.

ABSTRACT

Thirteen tests were carried out to investigate the effect of outwards eccentricity on the punching resistance of flat slab edge column connections. The slabs measured 2350 mm (92.5 in.) by 1700 mm (66.9 in.) on plan and were 180 mm (7.1 in.) thick. One end of the slab was supported on a 300 mm (11.8 in.) square column with a boot at its base for imposition of eccentricity. The other end was supported on a fixed roller support that extended across the full slab width of 1700 mm (66.9 in.). Four point loads were applied to the unsupported slab edges. The tested variables were eccentricity and the areas of flexural, shear and torsion reinforcement. Presented test results include reinforcement strains, displacements, rotations, crack patterns, failure modes and ultimate loads.

The ACI 318 design procedure for punching shear at edge columns with outwards eccentricity is shown to be overly conservative unless the interaction between punching shear and unbalanced moment is reduced as permitted by the code. The EC2 design procedure is unsatisfactory and a modification is proposed.

Keywords: flat slab; edge columns; punching shear; outward eccentricity; slab column connections.

INTRODUCTION

Outwards eccentricity can arise at flat slab to edge column connections subject to wind and seismic loading. Although design standards make recommendations for the design of external slab column connections with outward eccentricity, there are very few published experimental data to verify their recommendations. Previous research[1-7] into the behavior of flat slab to edge column connections has focused almost entirely on connections with inwards eccentricity with respect to the column centerline. Up to now, outwards eccentricity has been almost completely neglected with the exception of two tests by Narasimhan[8] of which one had a shear hat consisting of a single perimeter of inclined stirrups. Notably, Stamenković and Chapman[9] tested internal, edge and corner connections with systematically varying inward eccentricities. They examined the influence of moment transfer on punching resistance and found that at edge columns the interaction depends on the orientation of the moment axis with respect to the slab edge. They found the interaction between punching shear and flexural resistance to be linear, as for internal slab column connections, when the axis of bending is perpendicular to the slab edge but almost square for “normal” moments where the axis of bending is parallel to the slab edge. Subsequently, Regan[10] and Moehle[11], whose research informs EC2[12] and ACI 318[13] respectively, determined conditions under which interaction between normal bending and shear can be neglected at edge columns. The present research provides the first systematic study of the effect of outwards eccentricity on the punching resistance of edge column slab connections.

RESEARCH SIGNIFICANCE

The influence of outwards eccentricity on punching resistance at edge columns is virtually unexplored. This is a significant omission as outwards eccentricity can arise in flat slab buildings under lateral loading from winds and earthquakes. The paper provides experimental data for assessing and improving design methods for punching. Analysis of the test results demonstrates the necessity of accounting for redistribution between flexure and shear when accounting for the effect of uneven shear at edge column connections. The ACI 318[13] provisions for punching shear are shown to be adequate for outwards eccentricity unlike those of EC2[12] where a modification is proposed.

EXPERIMENTAL INVESTIGATION

Test Specimens

Thirteen large scale specimens were tested with the geometry and support conditions shown in **Fig. 1**. The column was supported on a stub projection which was oriented in the direction of the required eccentricity. All the eccentricities reported in this paper are measured from the column centerline with outwards eccentricity being defined as positive. **Table 1** shows the characteristics of the tested slabs. The first six specimens, L1 to L6, had the same geometry and reinforcement arrangements and were unreinforced in shear. These tests investigated the effect on punching resistance of systematically varying eccentricity from 300 mm (11.8 in.) inwards to 400 mm (15.7 in.) outwards. The bottom flexural reinforcement was increased in tests L7, L11 and L12 to enhance the flexural resistance under large outwards eccentricities. Torsional reinforcement in the form of closed stirrups was provided in the slab edge of specimens L8 and L13. Slabs L9 and L10 were reinforced with punching shear reinforcement and were tested with 0 and 200 mm (7.9 in.) outwards eccentricity respectively.

Concrete

The slabs were cast from ready-mix concrete with a nominal compressive strength of 40 MPa (5800 psi). Crushed limestone sand and gravel were used as aggregate, with 9.5 mm (0.4 in.) maximum size of coarse aggregate. The concrete compressive strength, splitting strength and elastic modulus were determined for each slab by testing cylinders measuring 100 mm (3.9 in.) in diameter by 200 mm (7.9 in.) long. A total of nine cylinders, three for each type of test, were tested at the same time as the corresponding slabs. The resulting mean material properties are listed in **Table 1**. The reported strengths are as measured with no conversion to equivalent 300 mm × 150 mm cylinder strengths.

Reinforcement

The reinforcement material properties are listed in **Table 2**. **Fig. 2** shows the reinforcement arrangement adopted in slabs L1 to L6 and L9 which is depicted "standard". The standard flexural reinforcement was designed to study punching failure in slabs close to flexural failure at the column face. The ends of the flexural reinforcement were anchored with hooks. The bottom flexural reinforcement was enhanced as shown in **Fig. 3a** for slabs L7 and L10 to L13 and **Fig. 3b** for slab L8 in order to increase the flexural capacity at the column face which was close to governing in the tests with standard reinforcement. The top flexural reinforcement of the slabs in **Fig. 3** was unchanged from the "standard" distribution apart from the provision of an additional transverse bar at the slab edge which was provided to increase the torsional resistance of the slab edge. The cover to the outer layers of top and bottom reinforcement was 20 mm (0.8 in.) in all the slabs. **Fig. 4a** shows the column stub reinforcement for slabs with both "standard" and "enhanced" flexural reinforcement. The column reinforcement was increased in the tests with enhanced flexural reinforcement in order that column failure was not critical. The column stirrups were 6.3 mm (0.25 in.) in diameter and spaced at 100 mm (3.9 in.) outside the slab depth.

Slabs L9 and L10 were reinforced with shear studs positioned in a radial arrangement as shown in **Fig. 4b**. The shear studs were 8 mm (0.3 in.) in diameter with 8 mm (0.3 in.) thick, 25 mm (1 in.)

diameter circular heads welded to each end. Additional 8 mm (0.3 in.) and 6.3 mm (0.25 in.) diameter closed ties, with the dimensions shown in **Fig. 4**c, were provided in slabs L8 and L13, respectively, as shown in **Fig. 3b** to increase the torsional resistance of the slab edge. The tie is opened in **Fig. 4c** to shows its anchorage details more clearly.

Test Setup and Procedures

The slabs were loaded incrementally to failure through an internal reaction frame which was anchored to the laboratory strong floor as shown in **Fig. 5**. The slabs were tested under monotonic static loading because the primary objective was to determine the influence of outwards eccentricity on punching resistance. Further research is required to determine the influence of cyclic loading from earthquakes on punching resistance. The slab was supported on a roller under the column boot. At the other end, it was supported on a fixed roller which extended across the full slab width. Vertical load was applied through two hydraulic jacks. Loads were measured with four hollow load cells that were attached to the tie rods that distributed the load equally between the four loading plates. Hard rubber pads were positioned between the loading plates and slab.

Instrumentation

Strains were measured in the top and bottom flexural reinforcement adjacent to the column with up to 30 electrical resistance strain gauges. The number and position of gauges varied between specimens as described by Albuquerque [(14)]. Strains were measured at mid-height of 16 shear studs in L9 and L10 as well as at the center of each leg of the four stirrups placed in the slab edge south of the column in L8 and L13. Surface strains were measured in the top and bottom surfaces of the slab around the column. Displacements were measured with 15 Linear Voltage Displacement Transducers (LVDTs) positioned as shown in **Fig. 6**. Rotations were derived from the measured displacements. At several stages throughout each test, cracks were marked and photographed. Only selected data are reported in this paper as full details are reported elsewhere [(14)].

CODE METHODS

This section briefly describes the design methods for punching in ACI 318 and EC2 as reference is made to these in the subsequent discussion of test results.

ACI 318-14

ACI 318 calculates the design shear stress v_{Ed} on a rectangular critical section of length b_o located at $0.5d$ from the column face where d is the average slab effective depth. The shear stress is calculated using Eq. (1):

$$v_{Ed} = \frac{V_{Ed}}{A_c} \pm \frac{\gamma_v M_{cg} c}{J_c} \qquad (1)$$

where V_{Ed} is the design shear force, $A_c = b_o d$, c is the distance from the centroid of the critical section to the point where the shear stress is calculated (measured perpendicular to the moment axis), M_{cg} is the design out of balance moment about the centroid of the critical section and J_c is analogous to the polar moment of inertia of the critical section. Part of the unbalanced moment about the centroid of the critical shear perimeter $\gamma_f M_{cg}$ is assumed to be resisted by flexure within a width $c_2 + 3h$ centered on the column, where h is the slab thickness, with the remainder $\gamma_v M_{cg}$ resisted by eccentric shear where $\gamma_v = (1 - \gamma_f)$. In general, the coefficient γ_f is given by:

$$\gamma_f = \frac{1}{1 + (2/3) \cdot \sqrt{b_1 / b_2}} \qquad (2)$$

where $b_1 = c_1 + 0.5d$ and $b_2 = c_2 + d$

However, based on research by Moehle[11], for edge columns with unbalanced moments about an axis parallel to the slab edge, ACI 318-14 allows γ_f to be taken as 1.0 at edge columns provided V_{Ed} is less than $0.75\phi V_c$ (where V_c is the shear resistance provided by concrete in the absence of unbalanced moment and ϕ is a capacity reduction factor which equals 0.75 for design), sufficient flexural reinforcement is available within c_2+3h to resist M_{cg} and the net tensile strain, calculated for the effective slab width of c_2+3h, is not less than 0.004. This strain limit is not applied in the analyses of this paper as in ACI 318-11. Taking γ_f as 1.0 is equivalent to neglecting interaction between punching and flexure and is questioned[15]. If the flexural resistance M_R, within c_2+3h, is insufficient to resist M_{cg}, the residual moment M_{cg} - M_R must be resisted by eccentric shear. In this case, the shear resistance can be shown to be:

$$V_R = \frac{\phi J_c V_{R0} + M_R A_c c_{\max}}{J_c + A_c c_{\max} e_{cg}} \tag{3}$$

where $e_{cg} = M_{cg}/V_{Ed}$ and c_{max} is the perpendicular distance to the most stressed extreme fiber of the control section.

MacGregor and Wight[16] show that J_c is calculated for edge columns with normal eccentricity as:

$$J_c = 2\left(\frac{b_1 d^3}{12}\right) + 2\left(\frac{d b_1^3}{12}\right) + 2 b_1 d\left(\frac{b_1}{2} - c_{AB}\right)^2 + b_2 d c_{AB}^2 \tag{4}$$

in which c_{AB} is the perpendicular distance from the centroid of the critical perimeter to its side parallel to the slab edge which is given by:

$$c_{AB} = \frac{b_1^2}{2b_1 + b_2} \tag{5}$$

The maximum allowable design shear stress on the critical section b_o is ϕv_R where for slabs without shear reinforcement, v_R is v_c which equals $1/3\sqrt{f_c}$ MPa ($4\sqrt{f_c}$ psi) for the tested slabs. For slabs with shear reinforcement, the shear resistance v_R is the sum of the resistances provided by the concrete v_c and shear reinforcement v_s. For headed stud shear reinforcement, v_c equals $0.25\sqrt{f_c}$ MPa ($3\sqrt{f_c}$ psi) and v_s equals $A_{st} f_y/(b_o s)$ where A_{st} is the total cross sectional area of studs in each perimeter, f_y is the stud yield strength and s the radial stud spacing. Additionally, the shear stress due to factored load and moment should not exceed $1/6\sqrt{f_c}$ MPa ($2\sqrt{f_c}$ psi) on a control section located at $d/2$ beyond the outermost line of shear reinforcement.

EC2-04

EC2 calculates punching shear stress on a control perimeter U_1 at $2d$ from the column face as shown in **Fig. 7a** for an external column. EC2 accounts for eccentricity by calculating the design shear stress v_{Ed} in terms of an enhanced shear force βV_{Ed}. Where the eccentricity perpendicular to the slab edge (resulting from a moment about an axis parallel to the slab edge) is toward the interior and there is no eccentricity parallel to the edge, EC2 considers shear stress to be uniformly distributed along the reduced control perimeter U_1^* depicted in **Fig. 7b**. In this case, β equals U_1/U_1^*. This rule is intended to limit the maximum design shear force sufficiently for the interaction between shear and flexure to be neglected and is analogous to taking $\gamma_f = 1$ in ACI 318. If the eccentricity perpendicular to the slab edge is outwards, the design shear stress is calculated along the full control perimeter U_1 using an enhanced design shear force βV_{Ed} in which:

$$\beta = 1 + k \cdot \frac{M_{cg}}{V_{Ed}} \cdot \frac{U_1}{W_1} \tag{6}$$

where M_{cg} is the design moment about the centroid of the control perimeter, V_{Ed} is the design shear force, $W_1 = \int_o^u |e| dl$ in which dl is a length increment of the control perimeter U_1. At rectangular internal columns, EC2 defines e as the distance of dl from the axis about which M_{Ed} acts. However, for edge columns e should be measured from the plastic centroid of U_1 because W_1 is associated with a plastic stress distribution. In this case, W_1 is calculated as follows for rectangular edge columns:

$$W_1 = c_1^2 + 4dc_1 \sin\phi + 16d^2\left(\cos\phi + \phi\sin\phi - \frac{\pi}{4}\sin\phi - \frac{1}{2}\right) + 2dc_2\left(1 - \sin\phi\right) \tag{7}$$

in which

$$\phi = \frac{c_2 + 2\pi d - 2c_1}{8d} \qquad (8)$$

The coefficient k in Eq. (6), which equals 0.6 for square loaded areas, is analogous to γ_v in ACI 318. In the absence of contrary guidance, the authors have assumed that the k values in Table 6.1 of EC2 are applicable to edge as well as interior columns. EC2 requires the bending moment at the column face M_{cf} to be resisted by reinforcement centered on the column within a width c_2+y where y is the perpendicular distance from the inner column face to the slab edge (i.e. c_1 for the tested slabs). However, it is common practice in the UK to increase this width to c_1+2y. Additionally, Appendix I (informative) of EC2 limits the maximum moment transferred to edge columns through flexure to $0.255(c_1+y)f_c d^2/\gamma_c$ to prevent over reinforcement. This limit was not applied in the analysis of the tested slabs but is critical for L11 to L13.

The shear resistance without shear reinforcement is given by:

$$v_c = 0.18k(100\rho f_c)^{1/3}/\gamma_c \qquad (9)$$

where $\rho = (\rho_{xl}\rho_{yl})^{0.5} \leq 0.02$ in which ρ_{xl} and ρ_{yl} are the flexural tension reinforcement ratios (top transverse and bottom longitudinal for the tested slabs with outwards eccentricity) $\frac{A_{sl}}{bd}$ within a width b equal to the column width plus $3d$ to each side and $k = (1 + (200/d)^{0.5}) \leq 2$. γ_c is the partial factor for concrete which equals 1.5.

The shear resistance within the shear reinforcement is given by:

$$V_R = 0.75 v_c U_1 d + 1.5\left(\frac{d}{s}\right) A_{st} f_{ytd,ef} \qquad (10)$$

in which $f_{ytd,ef} = 250 + 0.25d \leq f_{yd}$ where $f_{yd} = f_y/\gamma_s$ is the design yield strength of the shear reinforcement. The coefficient γ_s is a partial factor of 1.15.

The control perimeter U_{out} at which shear reinforcement is not required is given by:

$$U_{out} = \beta V_{Ed} / \left(v_{Rd,c} d \right) \tag{11}$$

The outermost perimeter of shear reinforcement should be placed at a distance not greater than 1.5d within U_{out}. The transverse spacing of the shear reinforcement in the outer perimeter should not exceed 2d in the calculation of U_{out}.

EXPERIMENTAL RESULTS AND DISCUSSION

General Observations

Table 1 summarizes the total loads applied at failure, the corresponding column reactions and the primary failure modes. The maximum possible failure load is limited by flexure which is critical for reinforcement in the longitudinal (x axis in **Fig. 1**) direction. Flexural failure arises as a result of either a yield line forming in the span across the full slab width or the formation of a localized yield line mechanism around the column. According to Regan[10], the total moment at the inner column face M_{cf} is made up of a "component M_f resisted by steel passing through the column face and two components each M_t resisted by steel distributed within a width r on either side of the column. The components M_t are eventually transmitted to the column through torsion on its side faces". Regan[10] showed that for inward eccentricity the projection r can be estimated, on the basis of a 45^o projection, as the perpendicular distance from the inner column face to the slab edge. The corresponding effective width is $2c_1 + c_2$ for the tested slabs where the column dimensions c_1 and c_2 are defined in **Fig. 1**. Regan[10] also suggested that r could be increased by the provision of torsion reinforcement in the slab edge. Similar recommendations are given by Moehle[11] and ACI-ASCE Committee 352[17].

Fig. 8a compares the normal bending moments (i.e. resisted by longitudinal reinforcement) at failure along slabs L1 to L6 with the available moment of resistance which was calculated at the column face assuming reinforcement to be effective if anchored within a 45^{o} projection of the inner column face as discussed above. Only hooked bars were included in this calculation with bars being considered anchored if the transverse bar in the radius of the bend of the tension leg was entirely contained within the 45^{o} projections. The flexural resistance in **Fig. 8a** was calculated assuming that the effective width over which the longitudinal reinforcement is effective increases linearly from 900 mm (35.4 in.) at the column face to the full slab width at the centerline of the nearest pair of loads. **Figs. 8b** and **c** show the influence of eccentricity on the ultimate column load V_u of the tested slabs with standard (see **Fig. 2**) and enhanced reinforcement (see **Fig. 3**) respectively. Column loads corresponding to flexural failure in the span (depicted span) and at the column face are also shown. The latter (depicted c_2+$2c_1$ and c_2+c_1) are shown for effective reinforcement widths, centered on the column, of i) c_2+$2c_1$, and anchored as described above (7 bars for slabs L1-L6, 8 bars for L8 and 10 bars for L7, L9-L13), and ii) c_2+ c_1 (5 bars for slabs L1-L6, 6 bars for L8 and 8 bars for L7, L9-L13) as adopted in EC2. **Figs. 8a** and **b** suggest that flexural failure occurred, or was imminent, in slabs L3 to L6 with standard reinforcement. Of these, L3 and L4 appeared to fail in flexure at the column face prior to subsequent punching whereas L5 and L6 failed in punching. **Figs. 8b** and **c** show that at eccentricities of 200 mm (7.6 in.) and above the measured punching resistance reduced with increasing outwards eccentricity almost identically to the calculated column load corresponding to flexural failure at the column face.

Comparison of the failure loads of slabs L4 and L7, with outward eccentricities of 400 mm (15.7 in.) and similar concrete strengths, shows that enhancing the flexural reinforcement in L7 increased the ultimate column load by 37%. Closed stirrups at the slab edge increased the column ultimate load of L8 by 11% relative to L7 and L13 by 17% compared with L11. The primary failure modes of slabs L7 and L8 are classified as flexural in **Table 1** though punching subsequently occurred with L8 failing in almost unidirectional shear across the full slab width owing to the strengthening effect of the torsional stirrups. **Fig. 8c** shows that the flexural resistance at the column face of slabs L8 and L13, which failed in punching, was increased by the torsional stirrups provided at the slab edge. Slabs 9 and 10 with shear studs failed in one way shear adjacent to the roller support but, as shown later, above the punching capacities given by ACI 318 and EC2. Slabs 11 and 12 failed locally under the loading plates, as a result of the loading plates being repositioned nearer the slab edge to avoid strain gauge cables, again at greater loads than predicted by ACI 318 and EC2.

Crack Patterns

Fig. 9 shows the crack patterns in tests L1 to L3 with eccentricities of 300 mm (11.8 in.) inwards, 0 and 300 mm (11.8 in.) outwards which are representative. In L1, the first cracks formed in the top surface of the slab perpendicular to the inside column face and progressed longitudinally towards mid-span. Almost parallel transverse cracks developed in the bottom surface of the slab. These cracks initially formed around the column perimeter with cracks subsequently forming in the span as the load was increased. Failure occurred by punching when concrete crushing was observed in the flexural compression zone at the face of the column.

The cracks in the top surface of L2, with zero eccentricity, were mainly longitudinal. The crack pattern in the top surface of the slab was fully developed at around 70% of the ultimate load and thereafter cracks primarily widened as the loads were increased to failure. Some of the cracks in the top surface penetrated the entire slab thickness. The crack pattern in the bottom surface of L2 was similar to L1 but cracks initially formed near mid-span with subsequent cracks forming progressively nearer the column unlike L1 where the sequence was reversed. Similar crack patterns developed in L3 and L4, with eccentricities of 300 mm (11.8 in.) and 400 mm (15.7 in.), respectively. Diagonal cracks formed in the bottom surface of L3 and L4 adjacent to the column sides at a similar orientation to those in the top surface of L1. Comparison of the crack patterns in the top surface of L1 and the bottom surface of L3 suggests that the effective width over which the flexural reinforcement was mobilized at the column face was greater for L3 with outwards eccentricity due to the beneficial of transverse flexural compression at the bottom of the slab. A punching cone developed at failure of L3 and L4, but subsequent to localized yielding of the bottom longitudinal and top transverse bars at the column faces. The crack patterns in L7 and L8 with 400 mm (15.7 in.) eccentricity and enhanced flexural reinforcement were similar to those shown in **Fig. 9c** for L3. Albuquerque(14) gives full details of the remaining crack patterns which have similar characteristics.

Deflections and rotations

Fig. 10 shows deflected profiles at the penultimate load increment in slabs L1 to L3 which are representative. The effect of eccentricity is more evident in **Fig. 11** which shows displacements in L1 to L7 at transducers 4 and 11 (see **Fig. 6**) which were greatest. The maximum displacement at any given load increases with increasing outwards eccentricity due to the increase in sagging bending moments and associated column rotation. The load deflection curves do not exhibit any significant horizontal plateaus which is indicative of shear failure although localized yielding of flexural reinforcement occurred as discussed later. **Fig. 12** shows the influence of eccentricity and reinforcement detailing on the relationship between the normal moment on the line of the inner column face and the rotation θ_{normal} of the slab, between transducers 1 and 2, relative to the column. **Fig. 12a** shows that the rotational stiffness (M_n/θ_{normal}) of L1 with 300 mm (11.8 in.) inwards eccentricity is significantly greater than L3 with the same but outwards eccentricity. Comparison of the moment rotation responses of L6, L3 and L4, all with standard reinforcement, shows that the rotational stiffness reduced with increasing eccentricity. The rotational stiffness is also seen to have been increased by enhancing the longitudinal flexural reinforcement. **Fig. 12b** shows that the addition of closed stirrups at the slab edge increased strength but not rotational stiffness.

Fig. 13 shows the relationship between the column load V and θ_{normal} which is of interest because the Critical Shear Crack Theory (CSCT) of Muttoni(18), relates shear resistance to rotation. **Fig. 13a** shows rotations for slabs L1 to L6 with standard reinforcement and **Fig. 13b** rotations for slabs with enhanced reinforcement. The rotations of slabs L1 and L9 were in the opposite direction to slabs with outwards eccentricity but are shown positive for comparative purposes. Rotations increased with increasing outwards eccentricity due to the combined effect of a) the increased moment at the column face and b) the reduction in slab-column connection rotational stiffness with eccentricity visible in **Fig. 12**. Also, **Fig. 13b** shows that enhancing the flexural reinforcement reduced θ_{normal} in slabs with the same eccentricity. **Fig. 14** shows the rotations of the slab relative to the column in the transverse direction which is calculated between transducers 7 and 9. The final measured normal and transverse rotations and the corresponding column load are listed in **Table 3** in which the greater of the two is highlighted in bold. The normal rotation was greatest in L1 with inwards eccentricity and slabs L7 and L8 with 400 mm (15.7 in.) outwards eccentricity. In all other cases, the transverse rotation was greatest. **Table 3** also shows that the rotations between transducers 7 and 11 were very similar to those between 7 and 9 in all slabs. This indicates that the slab edge remained almost straight as the slab deflected. Conversely, the rotations between transducers 2 and 4 were significantly less than between 2 and 3 due to the deflection of the slab. The influence of rotation on punching resistance is unclear from **Figs. 12** to **14** and requires further study.

Strains

Flexural Reinforcement - **Figs. 15a** and **b** show selected strains at failure, and their position, in the top transverse reinforcement of slabs L1 to L5 and L11 to L12 respectively. The strains in gauges 1 to 5 and 6 to 10, where present, are plotted in separate lines. Gauges were placed just to the side of the adjoining transverse reinforcement bar in order to avoid damage to the gauges during assembly of the reinforcement cage. The strains in each line tend to increase from the innermost gauge towards the slab edge with the greatest strains occurring at the column face where yielding typically occurred at gauge 1 adjacent to the slab edge. **Figs. 16a** and **b** show selected strains at failure in the bottom longitudinal bars of slabs L2 to L5 and L11 to 12 respectively. **Fig. 16a** shows that the reinforcement yielded at the column face in test L3 and was close to yield in L4. These observations are consistent with **Fig. 8** which shows yielding at the column face of L3 and L4. **Fig. 16b** shows that yielding occurred at the column face in L11 with 350 mm (13.8 in.) eccentricity but not L12 with 150 mm (5.9 in.) eccentricity which is also consistent with **Fig. 8c**. The strains were typically less in the line of gauges at the column face (gauges 1, 3, 6, 9, 11, 13) than in the span (gauges 2, 4, 7, 10, 12, 14) since the sagging moment increased with distance from the column face as shown in **Fig. 8a**. Outside the column width the strains in the bottom longitudinal reinforcement of slabs L11 and L12 were fairly uniform across the slab width and below yield.

***Strains in Torsion Reinforcement* - Fig. 17** shows strains measured in the top and outer legs of the four gauged stirrups in L13. Strains were greatest in the stirrup legs nearest the column and reduced with increasing distance from the column. The strains in the bottom leg which are not shown ranged from 1.9‰ to 0.8‰ compared with 4.6‰ to 0.8‰ for the top leg. The strains in the outside leg of the stirrups were greater than in the inside leg reaching a maximum of 3.9‰ compared to 1.9‰.

STRENGTH ASSESSMENT OF TESTED SLABS

The shear resistances of the tested slabs were evaluated with ACI 318-14, without and with γ_v reduced, and EC2-04 taking ϕ, γ_s and γ_c as 1.0. **Table 4** compares the measured and calculated column failure loads corresponding to punching V_{shear} and flexural failure in the span $V_{flex\ span}$ and at the column face $V_{flex\ col\ face}$. The latter was calculated assuming reinforcement to be effective at the column face if contained within a band of width c_2+2y = 900 mm centered on the column and anchored as previously discussed.

Table 4 shows that ACI 318-14 gives reasonable predictions of the measured strengths V_u if γ_v is reduced, even for the slabs with shear reinforcement which is not permissible according to ACI 318, and the strength is limited to $V_{flex\ col\ face}$. The calculated shear resistance is $0.75V_{R0}$ for all the slabs except L4 and L8 where it is given by equation (3) because insufficient flexural reinforcement was provided for γ_v to be reduced to zero. However, the measured strengths are significantly underestimated if γ_v is not reduced as suggested by Ghali et al.[15]. The EC2 shear resistances are very conservative when calculated with β from Eq. (6) as specified in the code for outwards eccentricity. **Figs. 18a** and **b** shows the ultimate shear stress distribution around the EC2 control perimeter of slabs L1 and L3 with 300 mm inwards and 300 mm outwards eccentricity respectively calculated with β from Eq. (6). Comparison of the two figures shows that the reduced perimeter U_1* of **Fig. 7b**, which is intended for inwards eccentricity, is inapplicable for outwards eccentricity where, contrary to inwards eccentricity, vertical shear is largely resisted along the perimeter sides perpendicular to the axis of bending. Consequently, the reduced perimeter U_{1out}* of **Fig. 7c**, which equals U_1* for square columns, is more appropriate for outwards eccentricity. **Table 4** shows that the reduced perimeter of **Fig. 7c** works well for the tested slabs but further studies are required to investigate the influence of column aspect ratio on the definition of U_{1out}*.

CONCLUSIONS

The test data presented in this paper forms the first systematic study of outwards eccentricity at flat slab to edge column connections. The ultimate column load of specimens with the "standard" flexural reinforcement used in tests L1 to L6 reduced with increasing outwards eccentricity almost in line with the flexural capacity at the column face calculated assuming reinforcement was effective if contained within a 45^o projection of the column sides. All these slabs ultimately failed in punching but the primary failure mode of L3 and L4 with eccentricities of 300 mm (11.8 in.) and 400 mm (15.7 in.) was flexure at the column face. Punching resistance was increased by enhancing the area of flexural reinforcement in the span and by providing closed stirrups and additional top and bottom transverse bars at the slab edge.

The measured shear strengths of the tested slabs were compared with the strengths given by ACI 318 and EC2. ACI 318 is overly conservative if γ_f is calculated with equation (2) but gives reasonable strength predictions if γ_v is reduced, even for slabs with shear reinforcement, with the exception of slabs L3 and L4 where it overestimates the flexural resistance of the slab column connection. EC2 is very conservative if the shear enhancement factor β is calculated with Eq. (6) as specified in the code. This is attributed to EC2 neglecting redistribution of unbalanced moments between shear and flexure in the calculation of the coefficient k in Eq. (6). The EC2 design method would be improved by either using a reduced control perimeter like that shown in **Fig. 7c,** or adopting the ACI 318 approach of neglecting interaction between shear and flexure but for V_{Ed} less than $0.75V_{Ro}$ rather than $0.75V_c$ as specified in ACI 318.

ACKNOWLEDGMENTS

The authors wish to express their gratitude to Paul E. Regan (ACI Member), Emeritus Professor of the University of Westminster - UK, for suggesting this research, and for all the support for the work being done in Brazil on Punching Shear. The authors wish also to express their gratitude to CNPq and CAPES, Brazilian Research Development Agencies, for supporting the work described in this paper. The support of Professor Y. Nagato during the tests is also acknowledged.

NOTATION

A_c = Cross sectional area of ACI 318 critical section

A_s = Area of flexural reinforcement

A_{st} = Area of shear reinforcement in each perimeter

b_0 = ACI 318 critical punching perimeter

b_1, b_2 = Dimensions of critical section b_0 measured perpendicular and parallel to slab edge

β = Enhancement factor for eccentric shear

c_1, c_2 = Column dimension perpendicular and parallel to the slab edge

c = Distance from centroidal axis of critical perimeter to point where shear stress is calculated.

d = Average effective depth of slab

e = Support eccentricity with respect to the column axis

e_{cg} = Support eccentricity with respect to centroid of control perimeter

ε_y = Yield strain of reinforcement

E_c = Concrete modulus of elasticity

E_s = Reinforcement modulus of elasticity

f_c = Compressive strength of concrete

f_{ct} = Tensile strength of concrete

f_y = Yield strength of reinforcement

$f_{ytd,ef}$ = Effective design strength of shear reinforcement

ϕ = ACI 318 strength reduction factor or bar diameter

γ_c, γ_s = Partial factors for concrete and steel

γ_v = Proportion of unbalanced moment transmitted by uneven shear

γ_f = Proportion of unbalanced moment transmitted by flexure

h = Slab thickness

J_c = Polar moment of inertia of critical section

k = Tabulated coefficient or Size effect factor

M_{cf} = Bending moment at inner column face

M_u = Ultimate bending moment about column centerline

M_{cg} = Design bending moment about centroid of control perimeter

M_R = Flexural resistance

P_u = Ultimate load in test

ρ = Reinforcement ratio

ρ_{xl}, ρ_{yl} = Flexural reinforcement ratio in x, y direction

θ_{normal} = Normal slab rotation relative to column

θ_{transv} = Transverse slab rotation relative to column

U_1 = Length of EC2 control perimeter

U_{1*} = Length of reduced EC2 control perimeter

U_{1out*} = Proposed reduced EC2 control perimeter for outward eccentricity

U_{out} = Length of outer control perimeter

v_R = Shear resistance

v_c = Shear resistance provided by concrete

v_{Ed} = Design shear stress

V_c = Punching resistance provided by concrete

V_{calc} = Least of V_{flex} and calculated punching resistance V_{shear}

V_{Ed} = Design shear force

V_{flex} = Column load corresponding to flexural failure

V_{R0} = Punching resistance in absence of unbalanced moment

V_R = Punching resistance

V_u = Experimental column load at failure

W_1 = Plastic modulus of EC2 control perimeter

y = Perpendicular distance from slab edge to inner column face

REFERENCES

1. Andersson, J. L. "Punching of Slabs Supported on Columns at Free Edges" (in Swedish). Nordisk Betong, Stockholm, 1966, pp. 179-200.

2. Kinnunen, S. "Tests on concrete slabs supported on columns at free edges". National Swedish Building Research Summaries R2:1971, Stockholm, 1971.

3. Zaghlool, E.R.F. "Strength and Behavior of Corner and Edge Column-Slab Connections in Reinforced Concrete Flat Plates", PhD Thesis, Dept. Civil Eng., Univ. of Calgary, 1971, 366p.

4. Hawkins, N. M.; W. G. Corley. "Moment Transfer to Columns in Slabs with Shearhead Reinforcement". *ACI Special Publication SP-42 - Shear in Reinforced Concrete*, 1974, pp. 847-879.

5. Mortin, J.D.; Ghali, A. "Connection of Flat Plates to Edge Columns". *ACI Structural Journal*, 88(2) 1991: 191–98.

6. El-Salakawy, E.F.; Polak, M.A.; Soliman, M.H. "Reinforced concrete slab-column edge

connections with shear studs". *Canadian Journal Civil Engineering*, V. 27, N°.2, 2000, pp. 338-348.

7. Sherif, A.; Emara, M.B.; Hassanein, A.; Magd, S.A. "Effect of the Column Dimensions on the Punching Shear Strength of Edge Column-Slab Connections", *ACI Special Public. 232*, Punching Shear in RC Slabs, 2005, pp. 175-192.

8. Narashiman, N. "Shear Reinforcement in Reinforced Concrete Column Heads", *PhD Thesis*, Imperial College, University of London, 1971.

9. Stamenković; A., Chapman, J.C. "Local Strength at Column Heads at Flat Slabs Subjected to a Combined Vertical and Horizontal Loading". *Proc. Institution of Civil Engin.* Part 2 London, 1974.

10. Regan, P. E. "Behaviour of reinforced concrete flat slabs" CIRIA Report 89, London, 1981, 90p.

8. Moehle J., "Strength of Slab-Column Edge Connections" ACI Struct. J. V85 No 1, 1988, 89-98.

9. Eurocode 2, "Design of Concrete Structures – Part 1-1: General Rules and Rules for Buildings", CEN, EN 1992-1-1, Brussels, Belgium, 2004, 225 pp.

10. ACI Committee 318, "Building Code Requirements for Structural Concrete (ACI 318M-14) and Commentary (ACI 318RM-14)", American Concrete Institute, Farmington Hills, MI, 2014, 519 pp.

14. Albuquerque, N. G. B., "Behavior of Connections between Reinforced Concrete Flat Slabs and Edge Columns with Inward and Outward Eccentricities" (in Portuguese). *PhD Thesis*, Civil Eng. Dept., Univ. Brasília, Brazil, 2014, 204 pp.

11. Ghali, A., Gayed, R. B. and Dilger W. "Design of Concrete Slabs for Punching Shear: Controversial Concepts". *ACI Structural Journal*, 112(4) 2015: 505-514.

12. MacGregor J.G., Wight J.K., "Reinforced Concrete - Mechanics and Design", 4th Ed, Prentice Hall, 2005, p.1111

13. Joint ACI-ASCE Comm. 352, 2011, "Guide for Design of SlabColumn Connect. in Monolithic Concrete Structures (ACI 352.1R-11)," American Concrete Institute, Farmington Hills, MI, 28 pp.

148. Muttoni, A. "Punching shear strength of reinforced concrete slabs without transverse reinforcement". *ACI Structural Journal*, 105(4) 2008: 440–450.

TABLES AND FIGURES

List of Tables:

Table 1 – Summary of test data

Slab	d (mm)	ρ[1] (%)	f_c (MPa)	f_{ct} (MPa)	E_c (GPa)	Reinforcement	e (mm)	Mode	P_u (kN)	V_u (kN)
L1	147	0.96	46.8	3.4	29.3	Standard	-300	Punch	437	308
L2	146	1.24	44.7	3.0	27.5	Standard	0	Punch	525	315
L3	146	1.24	45.1	3.1	27.1	Standard	300	Flexural	490	256
L4	146	1.24	46.0	3.3	28.5	Standard	400	Flexural	420	210
L5	146	1.24	51.4	4.1	31.8	Standard	100	Punch	654	374
L6	146	1.24	52.1	4.3	32.4	Standard	200	Punch	605	330
L7	146	1.49	50.0	3.7	31.3	Enhanced	400	Flexural	575	288
L8	146	1.49	50.5	3.9	31.4	Enhanced+TR[2]	400	Flexural	640	320
L9	146	1.24	57.6	3.2	28.1	Standard+SR[3]	0	Shear[5]	815	489
L10	146	1.49	59.3	3.6	30.6	Enhanced+SR[3]	200	Shear[5]	815	445
L11	146	1.49	43.1	3.1	31.1	Enhanced	350	Local[6]	615	304
L12	146	1.49	43.6	3.3	31.7	Enhanced	150	Local[6]	655	347
L13	146	1.49	44.1	3.4	32.1	Enhanced+TR[4]	350	Punch	700	357

Notes:

(1) $\rho = (\rho_{xl}\rho_{yl})^{0.5}$

(2) 8.0 mm torsion links

(3) Shear studs

(4) 6.3 mm torsion links

(5) Diagonal shear failure adjacent to roller support

(6) Local failure at loading plates which were marginally shifted to avoid strain gauge wires.

(7) 1 mm = 0.0394 in.; 1MPa = 145 psi.

Table 2 – Material properties of reinforcement

ϕ (mm)	A_s (mm^2)	ε_y (‰)	f_y (MPa)	E_s (GPa)
16.0	201.1	2.91	558	192
12.5	122.7	2.76	530	192
8.0	50.3	3.14	587	188
6.3	31.2	2.97	580	196

Notes:

(1) 1 mm = 0.0394 in.; 1 mm^2 = 0.00155 $in.^2$; 1MPa = 145 psi.

Table 3 – Final measured rotations of slab relative to column

Slab	**e (mm)**	**V_u (kN)**	**V_θ (kN)**	**θ_{normal} (Rad 10^{-3})**	**$\theta_{transv\ 7\text{-}11}$ (Rad 10^{-3})**	**$\theta_{transv\ 7\text{-}9}$ (Rad 10^{-3})**
L1	-300	308	308	**-8.49**	2.71	1.94
L2	0	315	315	1.26	6.53	**5.60**
L3	300	256	253	15.88	10.08	**10.94**
L4	400	210	208	6.61	6.65	**6.73**
L5	100	374	369	2.55	8.29	**8.05**
L6	200	330	330	12.07	12.40	**13.85**
L7	400	288	203	**9.23**	4.36	4.78
L8	400	320	243	**12.12**	5.95	5.56
L9	0	489	489	-0.76	-	**17.48**
L10	200	445	445	6.12	13.05	**14.60**
L11	350	304	304	13.50	14.23	**15.51**
L12	150	347	347	4.21	13.18	**14.04**
L13	350	357	268	10.97	11.28	**12.64**

Notes:

(1) 1 mm = 0.0394 in.; 1 kN = 0.2248 kip.

Table 4 – Calculated ultimate column loads of tested slabs

Slabs	V_u/V_{flex} col face	V_u/V_{flex} span	EC2: β Eq. (6) V_u/V_{shear} (1)	EC2: Proposed U_{1out}* V_u/V_{shear}	EC2: Proposed U_{1out}* V_u/V_{calc} (2)	ACI 318: V_u/V_{shear} γ_f Eq. (2)	ACI 318: V_u/V_c	ACI 318: V_u/V_{shear} γ_v *reduced*	ACI 318: V_{test}/V_{calc} (2)
L1	0.66	0.43	1.09	1.08	1.08	1.17	0.77	1.03	1.03
L2	0.43	0.71	1.63	1.04	1.04	1.32	0.81	1.08	1.08
L3	1.04	0.79	2.08	0.84	**1.04**	2.23	0.66	0.88	**1.04**
L4	1.04	0.71	1.90	0.69	**1.04**	2.13	0.53	0.86(3)	**1.04**
L5	0.83	0.94	2.20	1.18	1.18	1.99	0.90	1.20	1.20
L6	1.03	0.92	2.25	1.03	1.03	2.21	0.79	1.05	1.05
L7	1.03	0.74	2.39	0.86	**1.03**	2.80	0.70	0.94	**1.03**
L8	1.39	0.82	2.64	0.95	**1.39**	3.09	0.78	1.16(3)	**1.39**
L9	0.47	1.08	2.00	1.28	1.28	1.93	1.19	1.59	1.59
L10	0.99	0.94	2.42	1.12	1.12	2.99	1.07	1.42	1.42
L11	1.01	0.76	2.50	0.95	**1.01**	2.95	0.80	1.07	1.07
L12	0.69	0.72	2.19	1.08	1.08	2.28	0.91	1.21	1.21
L13	1.19	0.89	2.92	1.11	**1.19**	3.42	0.93	1.24	1.24
Average			2.17	1.02	1.12	2.35	-	1.13	1.18
St deviation			0.46	0.16	0.11	0.68	-	0.21	0.18

Notes:

(1) V_{shear} is calculated punching resistance

(2) Greatest of V_u/V_{shear}, $V_u/V_{flex\ col\ face}$, $V_u/V_{flex\ span}$ (flexural failure highlighted in bold)

(3) Eq. (3) governs punching resistance

(4) 1 mm = 0.0394 in.; 1 kN = 0.2248 kip.

List of Figures:

Fig. 18 – Shear stresses around U_1 for: (a) Slab L1 (e = 300 mm inwards); (b) Slab L3 (e = 300 mm outwards)

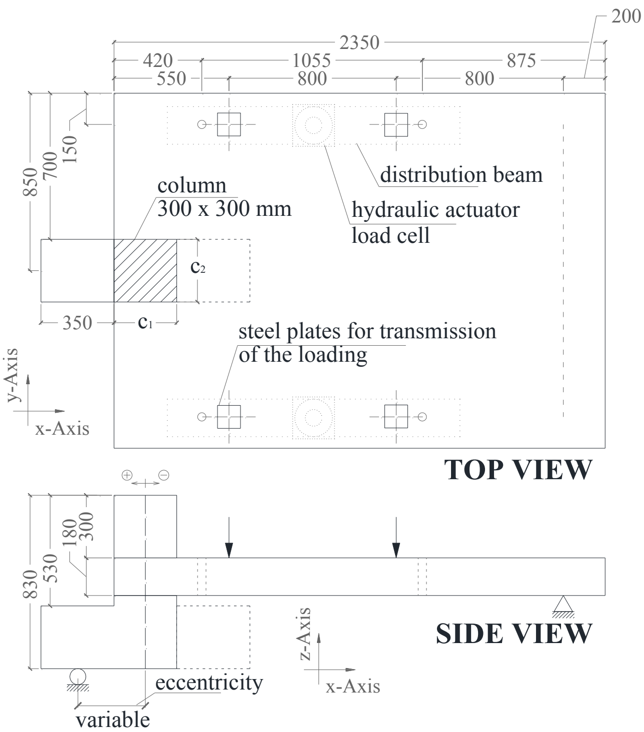

Fig. 1 – Plan showing positions of loads and reactions (Note: Dimensions in mm; 1 mm = 0.0394 in.)

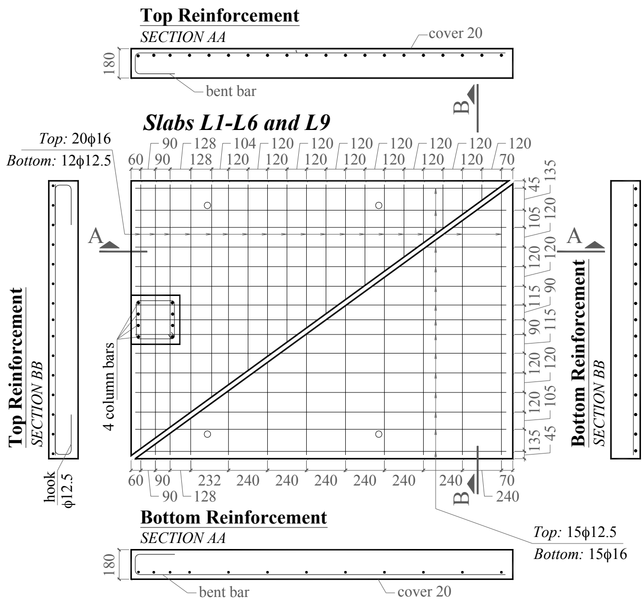

Fig. 2 – Standard distribution of flexural reinforcement (Note: Dimensions in mm; 1 mm = 0.0394 in.)

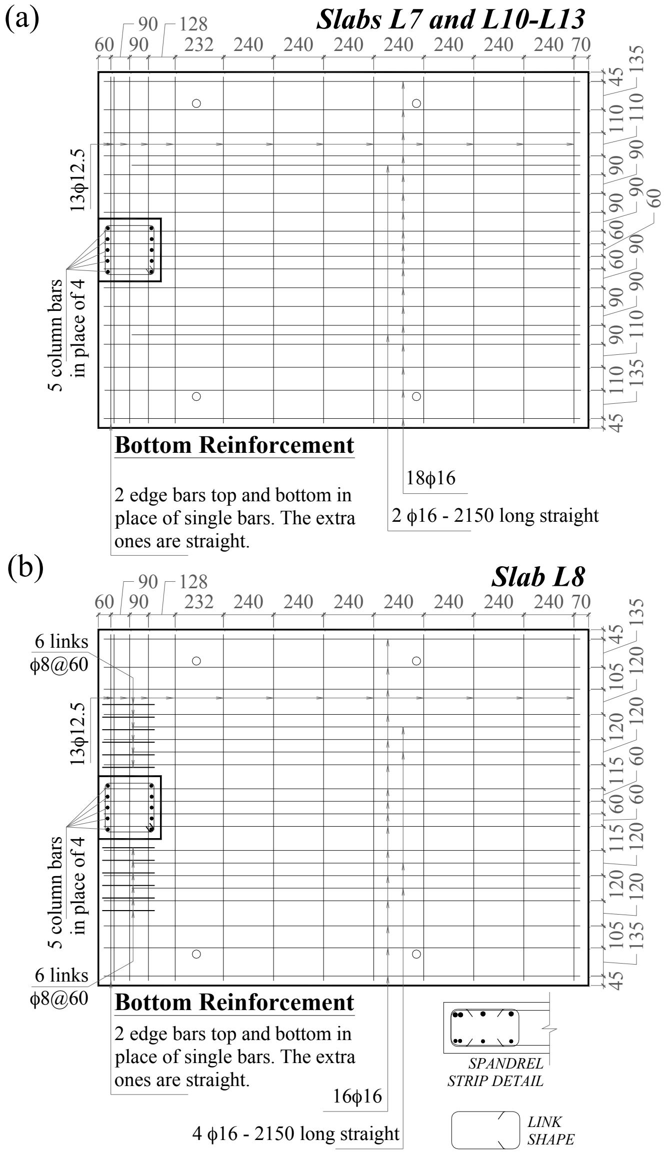

Fig. 3 – Enhanced distribution of flexural reinforcement: (a) Slabs L7 and L10 to L13; (b) Slab L8 (Note: Dimensions in mm; 1 mm = 0.0394 in.)

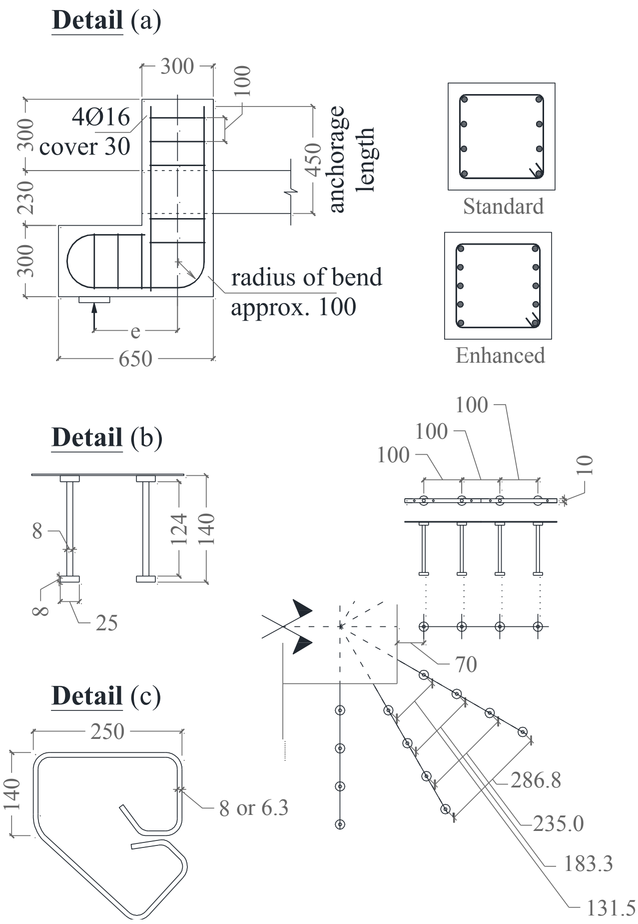

Fig. 4 – Details: (a) Column reinforcement; (b) Shear reinforcement (double-headed studs); (c) Torsion reinforcement (closed ties) (Note: Dimensions in mm; 1 mm = 0.0394 in.)

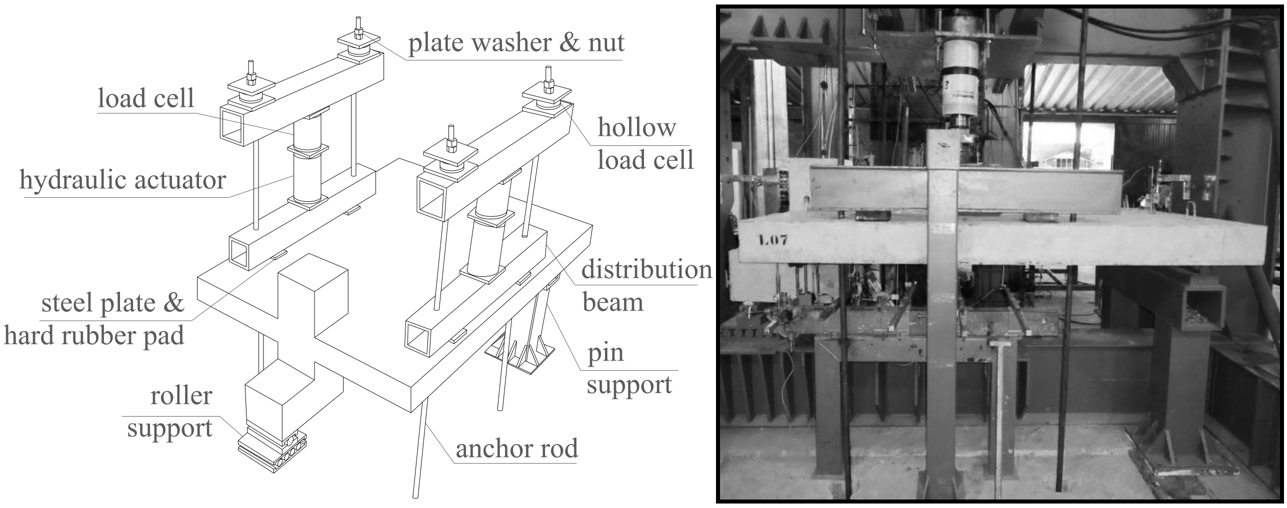

Fig. 5 – View of test set-up

1

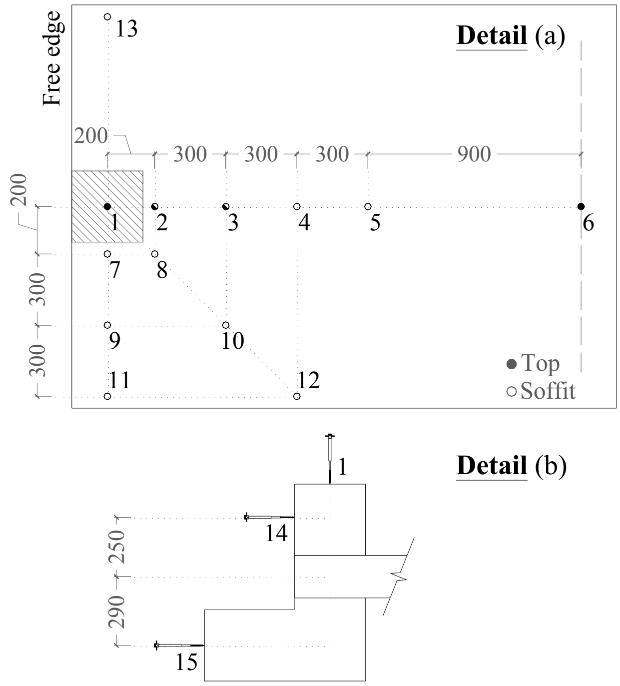

Fig. 6 – Arrangement of LVDTs for all specimens: (a) Plan; (b) Elevation (Note: Dimensions in mm; 1 mm = 0.0394 in.)

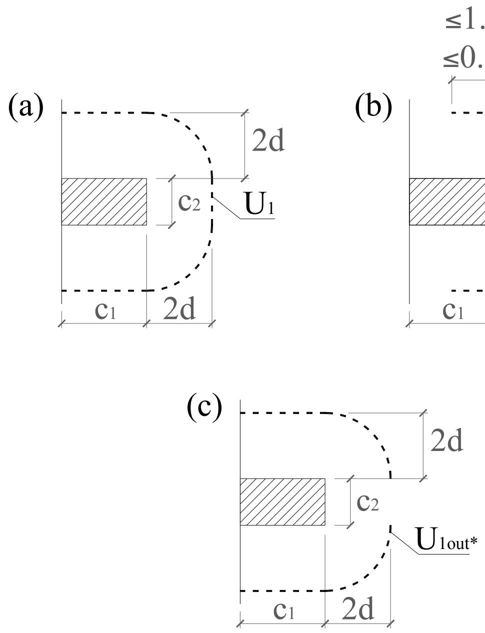

Fig. 7 – EC2 control perimeters at edge columns: (a) U_1; (b) reduced perimeter U_1*; (c) suggested reduced perimeter U_{1out}* for outwards eccentricity

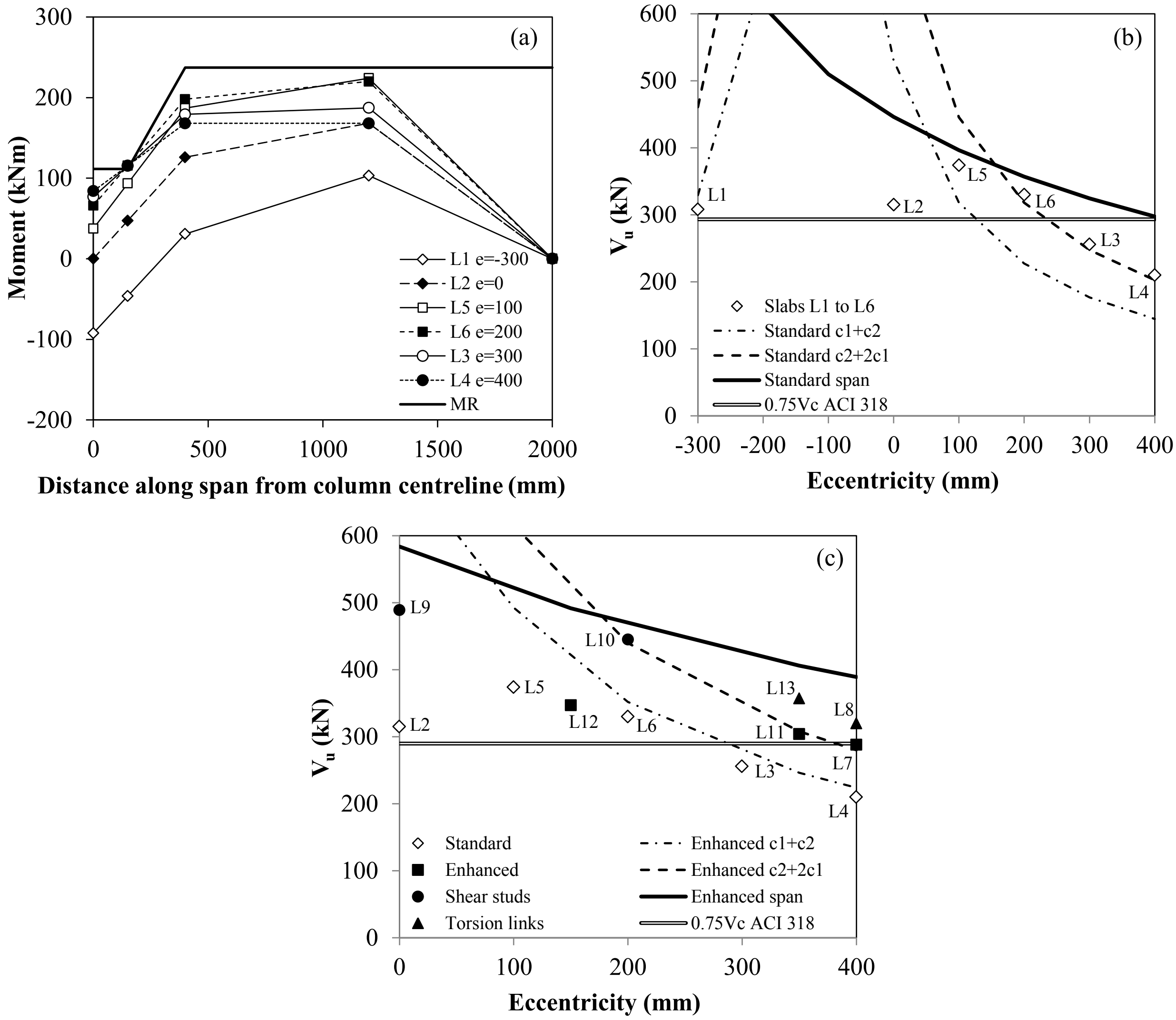

Fig. 8 – Influence of eccentricity on: (a) Bending moments at failure; (b) Shear resistance of slabs L1 to L6; (c) Shear resistance of slabs L7 to L13 (Note: 1 mm = 0.0394 in.; 1 kN = 0.2248 kip)

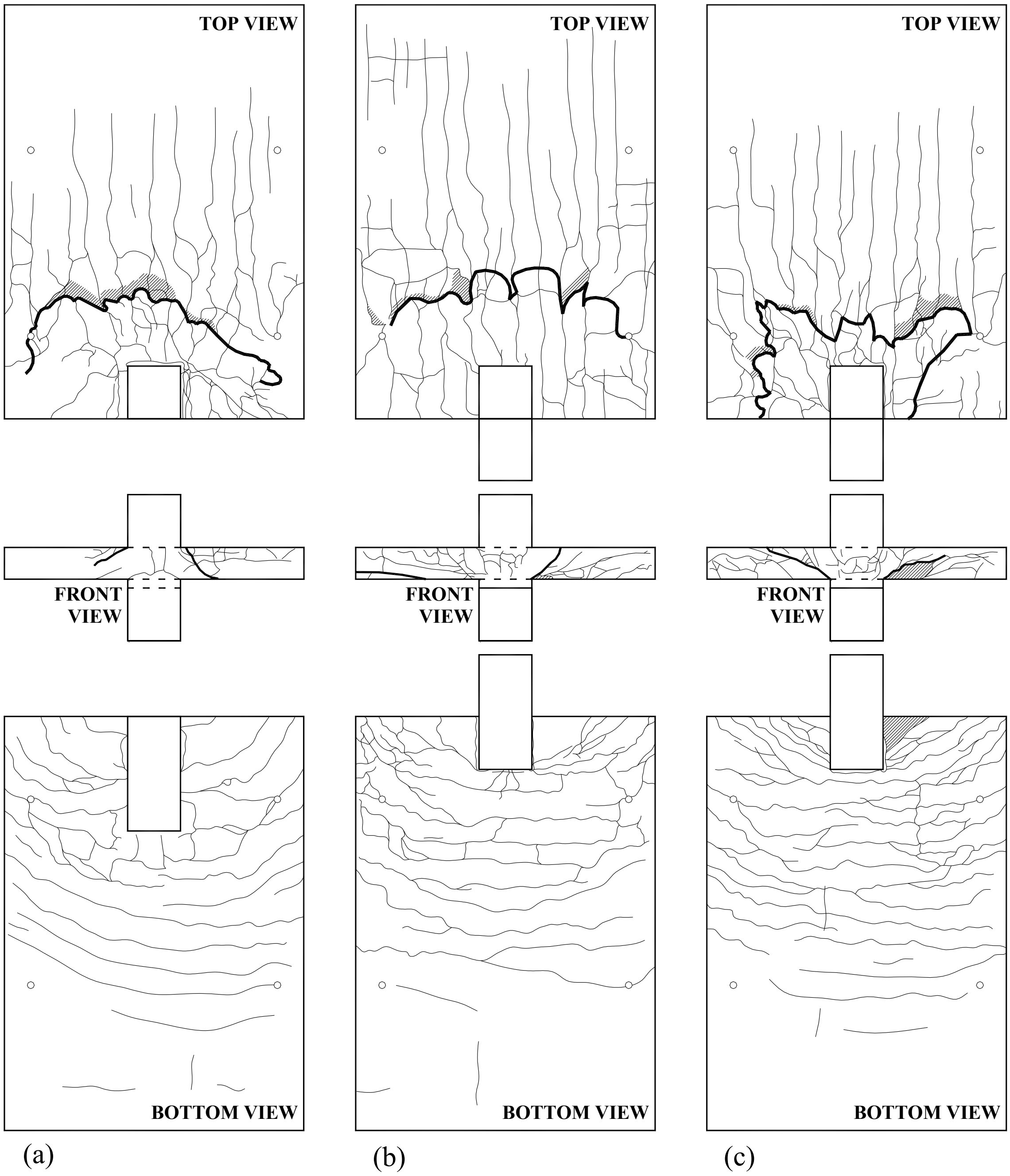

Fig. 9 – Cracking patterns: (a) Slab L1; (b) Slab L2; (c) Slab L3

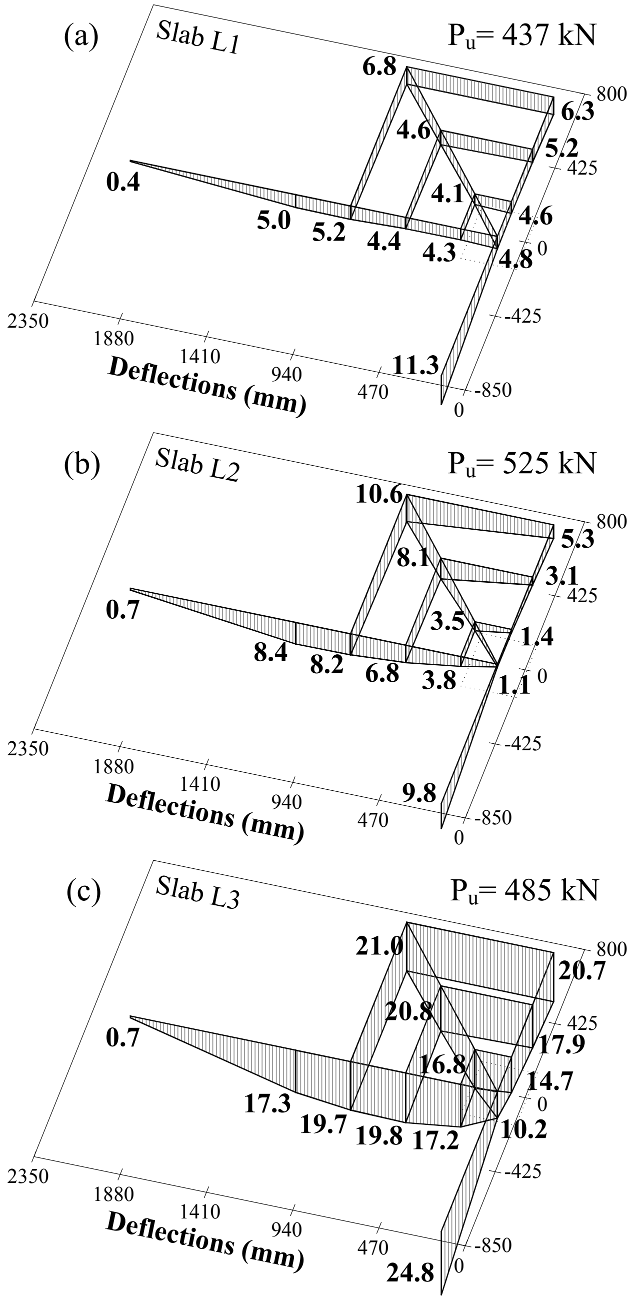

Fig. 10 – Deflected profiles: (a) Slab L1; (b) Slab L2; (c) Slab L3 (Note: Deflections in mm; 1 mm = 0.0394 in.; 1 kN = 0.2248 kip)

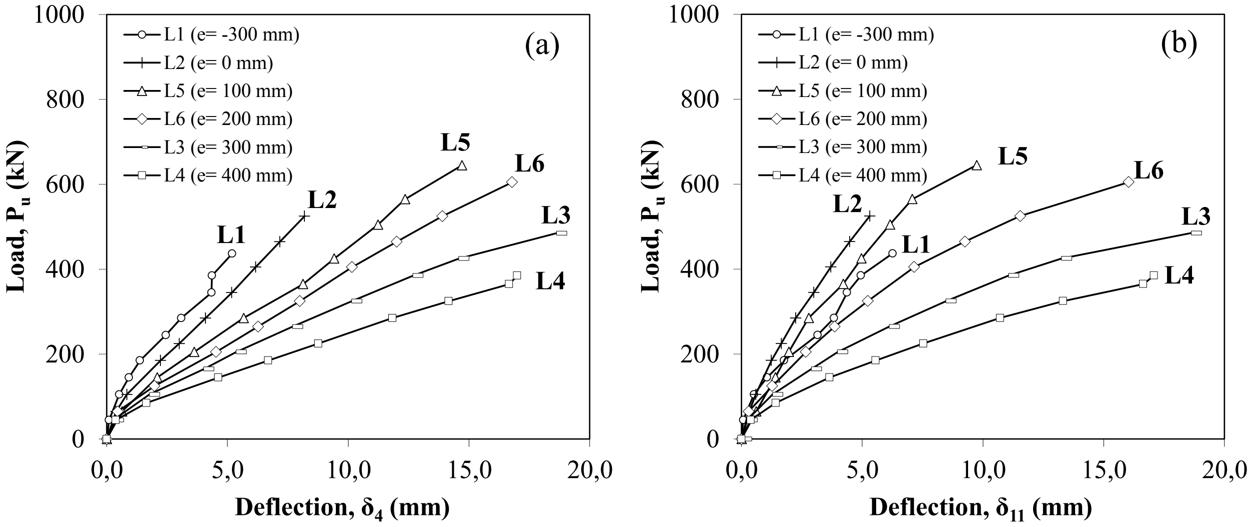

Fig. 8 – Load-deflection behavior: (a) LVDT 4; (b) LVDT 11 (Note: Displacements in mm; 1 kN = 0.2248 kip)

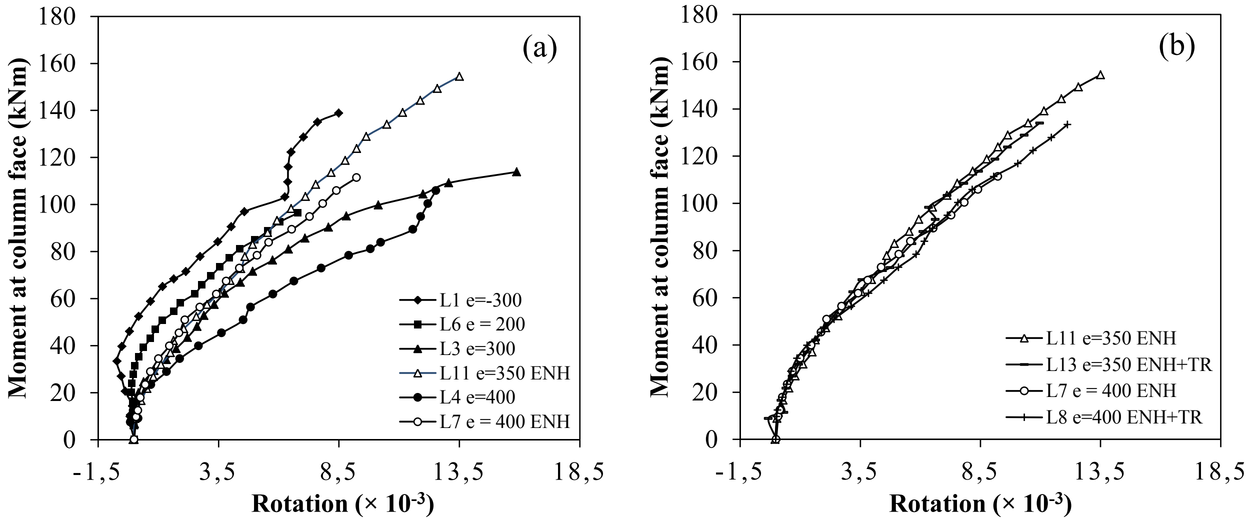

Fig. 9 – Relationship between normal slab rotations relative to column and moment at column face: (a) Influence of eccentricity; (b) Influence of torsion reinforcement (Note: Rotations in radians × 10^{-3}; 1 kN = 0.2248 kip, 1 kN.m = 0.7375 kip.ft)

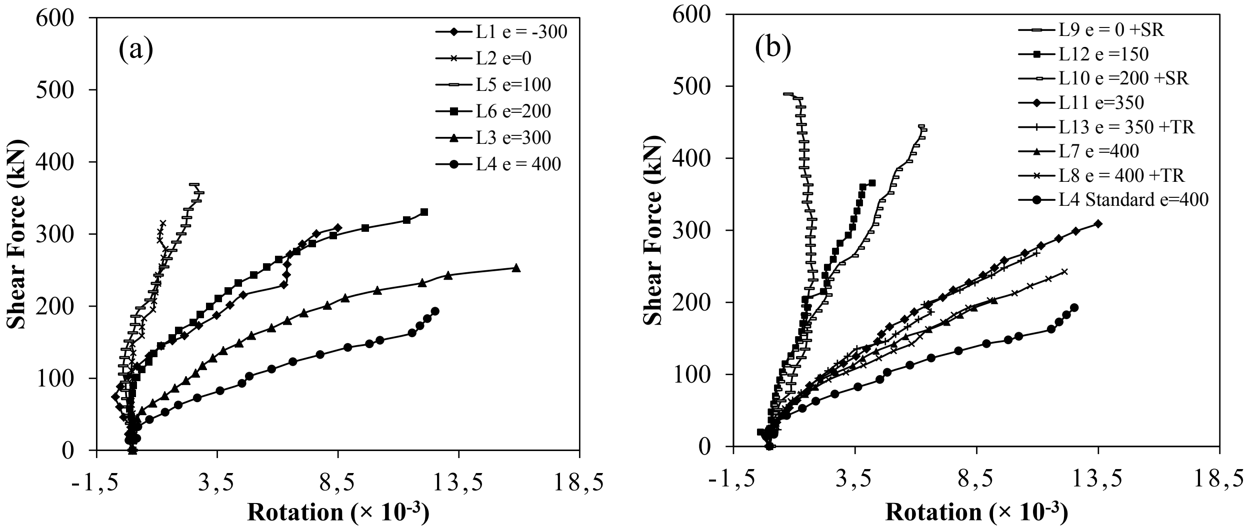

Fig. 10 – Influence of shear force on normal slab rotations relative to column: (a) Slabs L1 to L6; (b) Slabs L4 and L7 to L13 (Note: Rotations in radians × 10^{-3}; 1 kN = 0.2248 kip)

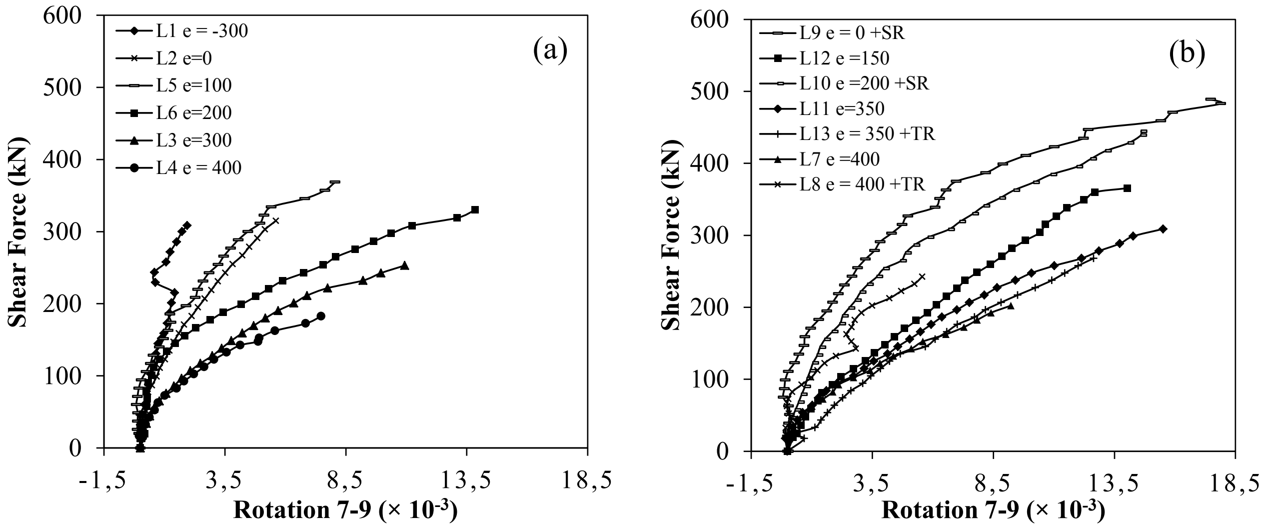

Fig. 11 – Influence of shear force on transverse slab rotations relative to column: (a) Slabs L1 to L6; (b) Slabs L3, L4, L6 to L13 (Note: Rotations in radians × 10^{-3}; 1 kN = 0.2248 kip)

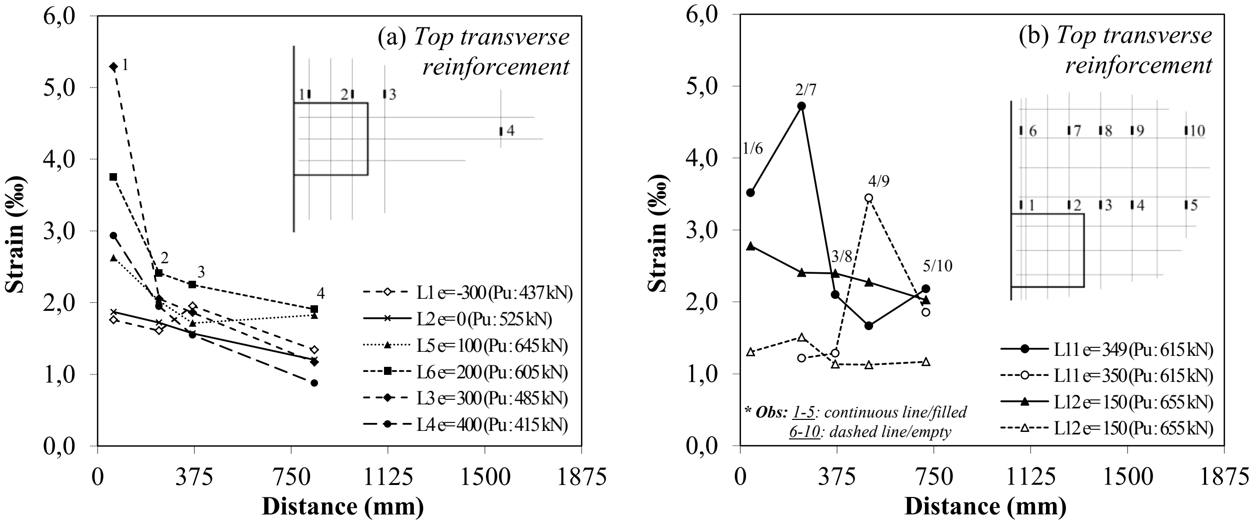

Fig. 12 – Strains in transverse flexural reinforcement: (a) Slabs L1 to L4; (b) Slabs L11 to L12

(Note: Strains in mm/m; 1 kN = 0.2248 kip)

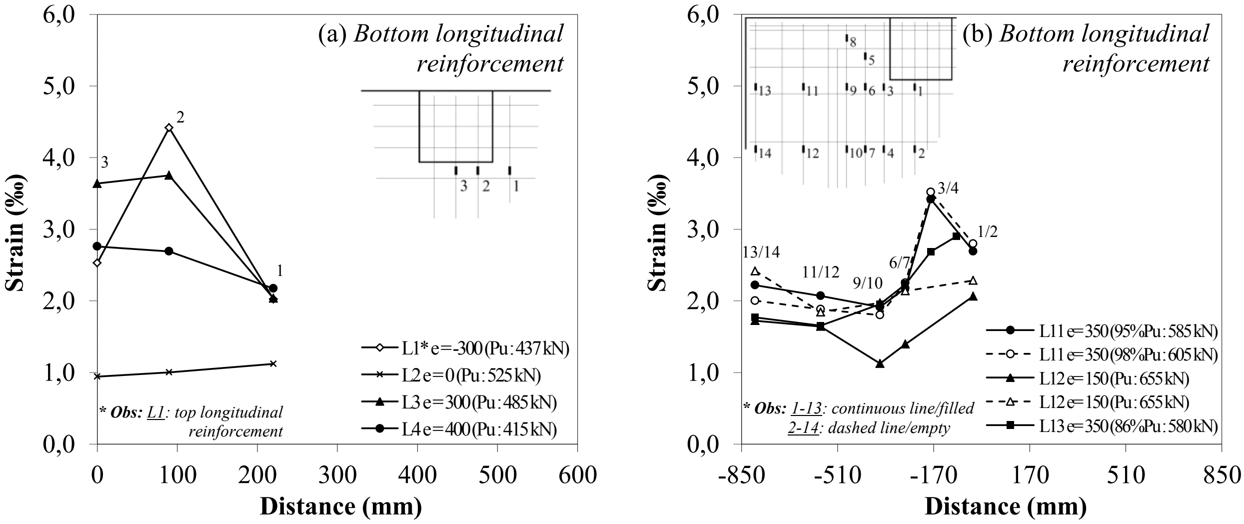

Fig. 13 – Strains in longitudinal flexural reinforcement: (a) Slabs L1 to L4; (b) Slabs L11 to L12 (Note: Strains in mm/m; 1 kN = 0.2248 kip)

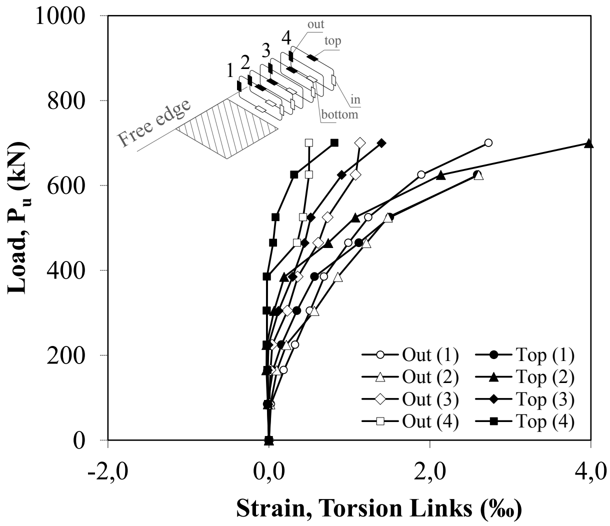

Fig. 14 – Strains in torsion reinforcement of slab L13 (Note: Strains in mm/m; 1 kN = 0.2248 kip)

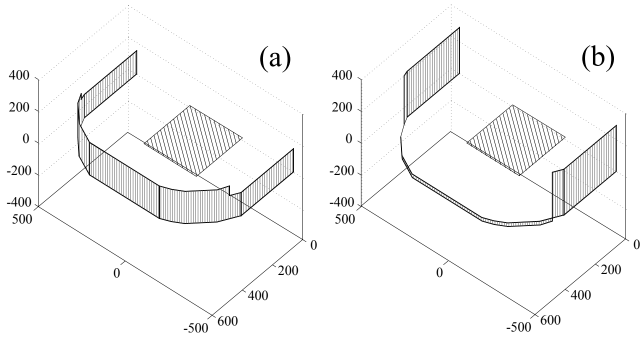

Fig. 15 – Shear stresses around U_1 for: (a) Slab L1 (e = 300 mm inwards); (b) Slab L3 (e = 300 mm outwards)